

## Real-Time Water Quality Modeling with Ensemble Kalman Filter for State and Parameter Estimation in Water Distribution Networks

Rajakumar, Anjana G.; Mohan Kumar, M. S.; Amrutur, Bharadwaj; Kapelan, Zoran

**DOI**

[10.1061/\(ASCE\)WR.1943-5452.0001118](https://doi.org/10.1061/(ASCE)WR.1943-5452.0001118)

**Publication date**

2019

**Document Version**

Accepted author manuscript

**Published in**

Journal of Water Resources Planning and Management

**Citation (APA)**

Rajakumar, A. G., Mohan Kumar, M. S., Amrutur, B., & Kapelan, Z. (2019). Real-Time Water Quality Modeling with Ensemble Kalman Filter for State and Parameter Estimation in Water Distribution Networks. *Journal of Water Resources Planning and Management*, 145(11), Article 04019049. [https://doi.org/10.1061/\(ASCE\)WR.1943-5452.0001118](https://doi.org/10.1061/(ASCE)WR.1943-5452.0001118)

**Important note**

To cite this publication, please use the final published version (if applicable). Please check the document version above.

**Copyright**

Other than for strictly personal use, it is not permitted to download, forward or distribute the text or part of it, without the consent of the author(s) and/or copyright holder(s), unless the work is under an open content license such as Creative Commons.

**Takedown policy**

Please contact us and provide details if you believe this document breaches copyrights. We will remove access to the work immediately and investigate your claim.

1       **REAL-TIME WATER QUALITY MODELLING WITH ENSEMBLE**  
2       **KALMAN FILTER FOR STATE AND PARAMETER ESTIMATION IN**  
3       **WATER DISTRIBUTION NETWORKS**

4       **G R Anjana<sup>1</sup>, M S Mohan Kumar<sup>2\*</sup>, Bharadwaj Amrutur<sup>3</sup> and Zoran Kapelan<sup>4,5</sup>**

5       <sup>1</sup>Research Scholar, Department of Civil Engineering, Indian Institute of Science, Bangalore,  
6       India.

7       E-mail: [anjanagr@iisc.ac.in](mailto:anjanagr@iisc.ac.in)

8       <sup>2</sup>PhD, Professor, Department of Civil Engineering, ICWaR, RBCCPS and IFCWS, Indian  
9       Institute of Science, Bangalore, India.

10      E-mail: [msmk@iisc.ac.in](mailto:msmk@iisc.ac.in)

11      <sup>3</sup>PhD, Professor, Robert Bosch Center for Cyber-Physical Systems (RBCCPS) and  
12      Department of Electrical Communications Engineering, Indian Institute of Science,  
13      Bangalore, India.

14      E-mail: [amrutur@iisc.ac.in](mailto:amrutur@iisc.ac.in)

15      <sup>4</sup>PhD, Delft university of Technology, Faculty of Civil Engineering and Geosciences,  
16      Department of Water Management, Delft, The Netherlands.

17      E-mail: [Z.Kapelan@tudelft.nl](mailto:Z.Kapelan@tudelft.nl)

18      <sup>5</sup>University of Exeter, College of Engineering, Mathematics and Physical Sciences, Exeter,  
19      United Kingdom.

20      E-mail: [Z.Kapelan@exeter.ac.uk](mailto:Z.Kapelan@exeter.ac.uk)

21      \*Corresponding author: M.S. Mohan Kumar ([msmk@iisc.ac.in](mailto:msmk@iisc.ac.in))

22

23

24

25 **Abstract**

26 This study presents a novel approach for real time water quality state (chlorine concentration)  
27 and reaction parameter estimation in Water Distribution Systems (WDS) using Ensemble  
28 Kalman Filter (EnKF) based data assimilation techniques. Two different types of EnKF based  
29 methods are used in this study: (a) Non-Iterative Restart-EnKF (NIR-EnKF) and Iterative  
30 Restart-EnKF (IR-EnKF). Use of these data assimilation frameworks for addressing key  
31 uncertainties in water quality models such as (i) uncertainty in the source or initial  
32 concentration of chlorine and (ii) uncertainty in wall reaction parameter, is studied. The effect  
33 of ensemble size, number and location of measurement nodes, measurement error and noise  
34 are also studied extensively in this work. The performance of the methodology proposed is  
35 tested on two different water networks: (i) Brushy Plains Network; (ii) and a big, city-wide  
36 WDS, Bangalore inflow network. The results of the simulation study show that, both NIR-  
37 EnKF and IR-EnKF methods are appropriate for dealing with uncertainty in source chlorine  
38 concentration, whereas IR-EnKF method performs better than NIR-EnKF method in case of  
39 reaction parameter uncertainty.

40

41

42

43

44

45

46

47

## 48 **Introduction**

49 Advancement in engineering and nanotechnology has resulted in the development of several  
50 sensors that can log online water quality data such as residual chlorine, pH, electrical  
51 conductivity, dissolved oxygen etc. in Water Distribution Systems (WDS) (Suresh et al.  
52 2014). Installation of these online sensors help in safeguarding the WDS against accidental  
53 and intentional contamination (Hall et al.2007). But, deployment of these sensors at all the  
54 nodes of a WDS is not feasible, considering the cost that will be incurred in doing so. Hence,  
55 sensors are placed only at a few strategic locations in the WDS (Aral et al. 2009; Ostfeld et  
56 al. 2008; Hart and Murray2010, Simone et al. 2016). In such systems with limited sampling  
57 locations, data assimilation creates the best estimate of the system state at the non-  
58 measurement nodes. In this work, the main objective is to assimilate the real time chlorine  
59 concentration data from these sensors, in a water quality model, for estimating the water  
60 quality state and parameters of the WDS in real time.

61 In this work, water quality state refers to the chlorine concentration at all the nodes of the  
62 WDS. Traditional methods for nodal chlorine concentration estimation involve a well  
63 calibrated water quality simulation model. In literature, numerous alternate methods for state  
64 and parameter estimation methods are available. A few of them are, inverse modelling (Clark  
65 et al. 1993; Biswas et al.1993; Rossman et al. 1994; Munavalli and Kumar 2004 &2005),  
66 time series analysis (Rodriguez and Serodes 1998; Polycarpou et al. 2002; Bowden et al.  
67 2006; Gibbs et al. 2006) and soft computational methods such as neural networks, genetic  
68 algorithm, machine learning etc. (Rodriguez and Serodes1998; Baxter et al. 1999, 2001;  
69 Serodes et al. 2001; Milot et al. 2002; Maier et al. 2004; Gibbs et al. 2006; Bowden et al.  
70 2006; May et al. 2008; D D'Souza and Kumar 2010; Soyupak et al. 2011). Water quality  
71 models are sensitive to uncertainties in parameters like reaction coefficient, initial  
72 concentration, hydraulic model errors, structural errors, demand uncertainties etc. (May et al.

73 2008). Data assimilation techniques were found to perform better than inverse modelling  
74 approaches, even in presence various of system uncertainties. (Liu et al. 2012). Also, unlike  
75 most of the conventional methods, data assimilation methods are also capable of  
76 incorporating real time sensor data for estimating the system state and parameters, thereby,  
77 making it an efficient tool for real time modelling of dynamic systems (Hendricks Franssen  
78 and Kinzelbach 2008).

79 Application of data assimilation span across numerous scientific disciplines such as electrical  
80 systems (Beides and Heydt 1991; Doucet et al. 2001; Blood and Krough 2008), oceanic  
81 sciences (Park and Kaneko 2000; Carton and Giese 2008), meteorological/atmospheric  
82 sciences (van Loon et al. 2000; Kalnay 2003), groundwater (Dre'court et al. 2006; Hendricks  
83 Franssen et al. 2008) , gas and petroleum engineering (Benkherouf and Allidina 1988, Emarah  
84 Shabaik et al. 2002, Liu et al.2005), surface water quality (Pastres et al. 2003).

85 In WDS, existing applications of data assimilation techniques are mainly focused on  
86 hydraulic state estimation and event detection (Kang and Lansey 2009; Ye and Fenner 2010  
87 & 2013; Jung and Lansey 2014, Okeya et al. 2014). It was observed that, most of the  
88 techniques used for hydraulic state estimation involves a linear data assimilation technique,  
89 such as - Kalman Filter or Extended Kalman Filters etc. (Hutton et al. 2014) . Owing to the  
90 high non-linearly of the water quality models, these linear data assimilation models cannot  
91 be applied directly for water quality state estimation in WDS. Hence, in this study, Monte  
92 Carlo based Ensemble Kalman Filter (EnKF) (Burgers et al. 1998) was used for chlorine data  
93 assimilation . This method is applied to WDS under two different uncertainties : (i) Source  
94 concentration ( $C_0$ ) uncertainty , (ii) wall decay parameter uncertainty ( $k_w$ ). Two different  
95 variants of EnKF (non-iterative and iterative EnKF) were formulated in this study and these  
96 methods were altered to deal with the problem of model variable initialization at intermediate  
97 time steps by implementing the Restart technique (Geir et al. 2003). These methods were

98 tested on two WDS: (i) Brushy plains network (Rossman et al. 1994) (ii) and a big, city-wide  
99 WDS, Bangalore inflow network (Manohar and Mohan Kumar 2013). In this study, it is  
100 assumed that the hydraulic model of the WDS is fully calibrated and hence, the uncertainties  
101 related to pipe roughness coefficient and systems demands are not considered.

102 The main objectives of this study is to compare the two variants of EnKF for application in  
103 water quality state estimation under system parameter uncertainties. Different scenarios are  
104 tested for assessing the applicability of these data assimilation methods. These scenarios  
105 studied are : Scenario (i) : The source concentration value ( $C_0$ ), is considered uncertain;  
106 Scenario ii: The reaction parameter value ( $k_w$ ), is considered uncertain. For each of these  
107 scenarios, the following sub-scenarios are also studied in this work : Sub-scenario (a). the  
108 number of realizations ( $n$ ) are varied ; Sub-scenario (b). The number ( $m$ ) and location of  
109 sensors are varied, Sub-scenario (c), measurement error and measurement noise is  
110 considered, in order to understand the sensitivity of data assimilation model.

## 111 **Methodology**

112 The over-all methodology adopted in this study has two parts: (i) Hydraulic and water quality  
113 simulation and (ii) water quality data assimilation model.

## 114 **Water Quality Prediction Model**

115 In this study, the water quality simulation (i.e. prediction) model consists of hydraulic and  
116 chlorine reaction and transport components, modelled using EPANET (Rossman 2000). A  
117 mass balance equation based one directional advection- dominated transport and reaction  
118 kinetics is used for chlorine concentration modelling in WDS. The partial differential  
119 equation governing chlorine transport in a pipe is:

$$120 \quad \frac{\partial C_i(x,t)}{\partial t} + v_i \frac{\partial C_i(x,t)}{\partial x} - R[C_i(x,t)] = 0 \quad (1)$$

121 where,  $C_i(x, t)$  is the chlorine concentration at any point  $x$  within link  $i$ , at time  $t$ .  $v_i$  is the  
122 mean flow velocity of the water; and  $R[C_i(x, t)]$  is the reaction- rate expression. In this study,  
123 a first order wall and first order bulk reaction model is being used:

$$124 \quad R[C_i(x, t)] = -k_b C_i(x, t) - \frac{k_w k_f}{r_h(k_w + k_f)} C_i(x, t) \quad (2)$$

125 where,  $k_b$  is the first order decay rate constant in the bulk flow (1/day),  $k_w$  is the wall decay  
126 parameter (m/day),  $k_f$  is the mass-transfer coefficient (m/day) and  $r_h$  is the hydraulic radius of  
127 pipe (one half the pipe radius).

128 More details about water quality modelling in WDS is available in the literature (Biswas et al.  
129 1993; Clark et al.1993 & 1995; Hallam et al. 2002; Grayman et al. 1988; Munavalli and  
130 Kumar 2005; Rossman et al. 1994; Vasconcelos et al. 1997).

131 Accurate modelling of chlorine concentrations in a WDS needs accurate understanding of  
132 decay mechanisms in the bulk water and on the pipe walls. Uncertainty analysis of water  
133 quality models have established the wall decay coefficient as the most sensitive parameter for  
134 water quality model output (Pasha and Lansley 2010). The wall decay coefficient in a WDS  
135 depends on the diameter of the pipe, flow in the pipe, concentration of chlorine, pipe service  
136 age etc. (Al-Jasser 2007; Fisher et al. 2017), whereas the bulk decay parameter mainly  
137 depends on the source water properties, and it seldom varies unless there is change in the  
138 source water quality. Along with decay parameters for chlorine in WDS, the water quality  
139 model output is sensitive to the source concentration value as well. The source chlorine  
140 concentration ( $C_0$ ) is usually monitored in WDS, but in case of measurement errors or sensor  
141 failure, the estimate of chlorine concentration across the system might vary and will lead to  
142 under or overdosing of the disinfectant. Hence, in this study, we are dealing with two  
143 different system uncertainties in water quality model development: (i) uncertainty in the input  
144 data or in this case, source concentration of chlorine ( $C_0$ ) and (ii) uncertainty in the wall

145 reaction parameter for chlorine reaction in pipelines ( $k_w$ ). In this study, the uncertainties  
 146 related to the hydraulic model such as demand uncertainty, pipe roughness coefficient etc. are  
 147 not considered, since accounting for these uncertainties make the problem more complex, and  
 148 the EnKF based data assimilation methodologies adopted in this study cannot be directly  
 149 applied to deal with these uncertainties.

## 150 **Data assimilation for water quality state and parameter estimation**

151 Data assimilation involves estimating the state of a particular system based on the predictions  
 152 and observations leading up to the present time. EnKF (Evensen 1994; Burgers et al. 1998;  
 153 Evensen 2003), is a Monte Carlo implementation of the Bayesian update problem. EnKF is a  
 154 special case of Kalman Filter (Kalman 1960) which uses ensembles or stochastic realization  
 155 (with different parameter and initial condition values) for approximating the states of the  
 156 system. EnKF based data assimilation consists of two steps: (i) Prediction step and (ii)  
 157 Update step. In the prediction step, a forward simulation model is used to predict the system  
 158 state as in equation (3):

$$159 \quad x_{t+1}^i = f(x_t^i, u_t^i, \theta, t) + \omega_t, i = 1, \dots, n \quad (3)$$

160 According to equation (3), the  $x_{t+1}^i$  is the  $i^{\text{th}}$  ensemble member forecast at time  $t+1$ , and  $x_t^i$  is  
 161 the  $i^{\text{th}}$  updated ensemble member at time  $t$ . Here,  $f$  is the forward simulation model (in this  
 162 case, EPANET water quality model of the system).  $\omega_t$  is the process noise (assumed to be  
 163 zero in this study),  $\theta$  is the system parameters,  $u_t$  are the forcing data or the system inputs .  
 164 Ensembles of the forcing data ( $u_t^i$ ) are created by adding noise  $\varepsilon_t^i$ , sampled from a  
 165 distribution of mean zero and variance,  $\Sigma_t^u$ , to the input data  $u_t$ .

$$166 \quad u_t^i = u_t + \varepsilon_t^i, \quad \varepsilon_t^i \sim N(0, \Sigma_t^u) \quad (4)$$



167 The parameters in this study are: pipe roughness coefficient ( $C$ ), hourly demand multiplier  
 168 ( $d_m$ ), initial concentration of chlorine ( $C_0$ ), chlorine reaction parameters. Among the above  
 169 listed parameters,  $C$  and  $d_m$  are assumed to be known, hence can be classified as system input  
 170  $u$ . Additional inputs required for predicting the system states are the network boundary  
 171 conditions (tanks initial level, reservoir head etc.) and base demand values at the nodes. .

172 From  $x_{t+1}^{i-}$ , the predicted states of the system,  $\hat{y}_{t+1}^i$ , the predicted measurements are  
 173 computed as

$$174 \quad \hat{y}_{t+1}^i = h(x_{t+1}^{i-}, \theta) \quad (5)$$

175 where  $h$  shows the relationship between the system states, parameters and the  
 176 observations/measurements.

177  $y_{t+1}$  is the field observation at the  $t+1^{th}$  time step, for which ensembles are generated by  
 178 adding a noise,  $\lambda_{t+1}^i$ .

$$179 \quad y_{t+1}^i = y_{t+1} + \lambda_{t+1}^i, \lambda_{t+1}^i \sim N(0, \Sigma_{t+1}^y) \quad (6)$$

180 The forecasted states ensembles (equation 3) are updated using a linear correction equation  
 181 according to the standard Kalman filter (equation 7):

$$182 \quad x_{t+1}^i = x_{t+1}^{i-} + K_{t+1}(y_{t+1}^i - \hat{y}_{t+1}^i) \quad (7)$$

183 Here,  $K_{t+1}$  is the Kalman gain matrix which is estimated from the covariance matrices as  
 184 shown in equation 8 (Moradkhani et al.,2005):

$$185 \quad K_{t+1} = \Sigma_{t+1}^{xy} [\Sigma_{t+1}^{yy} + \Sigma_{t+1}^y]^{-1} \quad (8)$$

186 where,  $\Sigma_{t+1}^{xy}$  is the forecast cross covariance of a priori state estimate  $x_{t+1}^{i-}$  and prediction  
 187  $\hat{y}_{t+1}^i$ , and  $\Sigma_{t+1}^{yy}$  is the forecast error covariance of prediction  $\hat{y}_{t+1}^i$ . In equation (7), the term  
 188  $K_{t+1}(Y_t - \hat{Y}_t)$ , is the perturbation vector (Hendricks Franssen and Kinzelbach 2008). In

189 equation (3), one of the key assumption is that the system parameter  $\theta$  is deterministic. In  
 190 scenarios, where the parameters  $\theta$  are unknown or uncertain, non-iterative or iterative EnKF  
 191 methods need to be used. These methods enable estimation of the uncertain system parameter  
 192 along with states using the real time observations from the field. In this work, the system state  
 193 and the model parameters ( $C_0$  and  $k_w$ ) are updated using two ensemble-based data  
 194 assimilation methodologies: (i) Non-Iterative Restart EnKF (NIR-EnKF), and (ii) Iterative  
 195 Restart EnKF (IR-EnKF).

196 In non-iterative- EnKF method, the parameter and the system states are combined to form an  
 197 augmented state vector, which enable simultaneous estimation of states and parameters  
 198 (Naevdal et al. 2003; Hendriks Franssen 2008). Whereas, in an iterative-EnKF, first the  
 199 parameters are updated using the current system measurements, and the updated parameters  
 200 are used to predict and update the system states for the same time step (Moradkhani et al.  
 201 2005). In both non-iterative and iterative EnKF methods, after updating the system  
 202 parameter, the forward simulation model (equation 3) is restarted from  $t: 0$ . This technique of  
 203 starting the simulation from  $t :0$  is called Restart EnKF (Gu and Oliver 2007, Hendricks  
 204 Franssen and Kinzelbach 2008, Song et al., 2014). In this study, Restart procedure was  
 205 implemented to reduce the error in EnKF model output due to parameter and system  
 206 initialization during intermediate water quality time steps.

### 207 **Non-Iterative Restart EnKF**

208 As mentioned earlier, in this approach, the states and the parameters are updated jointly. If  
 209 there are  $N$  states and  $M$  parameters, the augmented state vector will be of size  $(N+M,I)$ .  
 210 Forecasted ensembles of system parameters are created by adding a noise  $\zeta_t^i$  with covariance  
 211  $\Sigma_t^0$  to the updated parameter value of the previous timestep.

$$212 \quad \theta_{t+1}^i = \theta_t^i + \zeta_t^i, \quad \zeta_t^i \sim N(0, \Sigma_t^0) \quad (9)$$

213 These forecasted parameter ensembles  $\theta_{t+1}^{i-}$ , are updated (equation 10) simultaneously with  
 214 the forecasted states  $x_{t+1}^{i-}$  (equation 7)

$$215 \quad \theta_{t+1}^i = \theta_{t+1}^{i-} + K_{t+1}^\theta (y_{t+1}^i - \hat{y}_{t+1}^i) \quad (10)$$

216 Here,  $K_{t+1}^\theta$ , is the Kalman gain for updating the model parameter.

$$217 \quad K_{t+1}^\theta = \Sigma_{t+1}^{\theta y} [\Sigma_{t+1}^{yy} + \Sigma_{t+1}^y]^{-1} \quad (11)$$

218 Here  $\Sigma_{t+1}^{\theta y}$  is the cross covariance of the predicted parameter and measurement ensembles.

219 Rest of the terms are same as that of EnKF. The state vector is updated using equation (8)  
 220 and the corresponding Kalman gain is calculated as in equation (9). In this method, after each  
 221 time step (after updating the states and parameter ensembles), the simulation is restarted from  
 222  $t:0$  [ i.e. Equation 3 is run from  $t: 0$  for this algorithm, making it a NIR-EnKF].

### 223 **Iterative Restart EnKF**

224 IR-EnKF involves sequential forecast and update of parameters, followed by forecast and  
 225 update of system states for a particular time period. In this method, the updated parameters  
 226 (calculated using equation (10)),  $\theta_{t+1}^i$ , are used to forecast the system states for the same time  
 227 step ( $t+I$ ) (Equation 12).

$$228 \quad x_{t+1}^{i-} = f(x_t^i, u_t^i, \theta_{t+1}^i, t) \quad (12)$$

229  $\theta_{t+1}^i$  is the updated parameters for the time step  $t+I$ . The a priori water quality state of the  
 230 system  $x_{t+1}^{i-}$ , is updated using the Kalman gain for state correction (Equation 8).

231 This two-step approach is supposed to limit the problems associated with the linearization of  
 232 the relation between parameters and the observations.

### 233 **Filter Inbreeding**

234 During data assimilation, if the number of realizations are small, there exists an error due to  
235 sampling, and it will be reflected in the error covariance matrix. When there are insufficient  
236 realizations to span the model state space, the estimated error covariance will degrade after  
237 each time step, and this process is known as Filter inbreeding (Houtekamer and  
238 Mitchell1998; Lorenc2003). Whitaker and Hamill (2002) had suggested that the perturbations  
239 introduced in observations can also result in filter inbreeding.

240 Different methods are available in the literature for mitigating filter inbreeding effects  
241 (Anderson and Anderson 1999; Hamill et al. 2000; Anderson 2007). In this study, a  
242 mitigation approach based on a damping factor  $\alpha$  is used to analyse the effect of measurement  
243 errors and measurement noise on the data assimilation model output. The value of  $\alpha$  varies  
244 between 0 and 1(Hendricks Franssen and Kinzelbach 2008), and the state update equation is  
245 modified as follows:

$$246 \quad x_{t+1}^i = x_{t+1}^{i-} + \alpha K_{t+1}^x (y_{t+1}^i - \hat{y}_{t+1}^i) \quad (13)$$

247 The data assimilation algorithms were implemented using the EPANET Toolkit in  
248 MATLAB.

## 249 **Case Studies**

250 The EnKF based data assimilation methodologies developed for water quality state  
251 estimation in WDS is tested and validated in two WDS: (i) Brushy plains WDS and (ii)  
252 Bangalore inflow network. This section provides details on the two networks used in this  
253 study.

### 254 **Case Study 1: Brushy Plains WDS**

255 This network has been used in various studies related to water quality and WDS hydraulics  
256 (Rossman et al.1994; Boccelli et al. 1998; Nilsson et al. 2005; May et al. 2008; Clark 2015).

257 Details of this WDS are available in Rossman et al. (1994), in which chlorine concentration  
258 data from 8 sampling nodes across the network can be found. The estimated bulk reaction  
259 coefficient value for this WDS was found to be -0.55 /day, and the wall reaction coefficient  
260 value was found to be in the range of -0.45 to -0.15 m/day. The source concentration of  
261 chlorine is maintained at 1.1-1.16 mg/L, injected at a constant rate at the pumping station.  
262 Fig.1 shows the schematic of Brushy Plains WDS. Eight nodes were selected as measurement  
263 nodes for this network (in accordance with earlier research carried out on this network,  
264 Rossman et al. (1994)). Those measurement nodes are: 3,6,10,11,19, 25, 28 and 34. Synthetic  
265 chlorine measurements were generated every 15 minutes for the total duration of simulation  
266 (16 hours). The hydraulic time step of the simulation was about 60 minutes.

267 Data assimilation was carried out for scenario (i) and scenario (ii). Sub-scenarios (a), (b) and  
268 (c) were also studied for this case study. For scenario (i) and scenario (ii), the initial  
269 ensembles of parameters ( $C_0$  and  $k_w$ ) were sampled from a normal distribution, respectively.  
270 Both NIR-EnKF and IR-EnKF were tested for their application under (i) uncertainty in  $C_0$   
271 value and (ii) uncertainty in  $k_w$  value, for this WDS.

272 For sub-scenario (a), various sizes of stochastic realizations ( $n$ ) ranging from 20 -100 were  
273 generated for studying the variation in model accuracy with ensemble sizes. Sub-scenario (b)  
274 is simulated by reducing the number of measurement nodes ( $m$ ). The number of measurement  
275 nodes ( $m$ ) in the system are varied from 4 to 8 nodes, there by varying the measurement  
276 density in the system from 22 to 11percent. Two different sets of measurements are studied,  
277 each with 4 data sets. Measurement set A consists of data from nodes 3,6, 10 and 11,  
278 concentrated near to the pumping station, and measurement set B consisting of data from  
279 nodes 19, 25, 28 and 34, concentrated near to the tank. Varying the measurement locations  
280 and the measurement density in the WDS gives an idea of its effect on data assimilation.

281 The model performance in the presence of measurement errors and Gaussian noise for  $n$ : 20  
282 is also studied in detail, using a damping factor  $\alpha$ .(scenario (c)). In the sub-scenarios (a) and  
283 (b), the measurements used were assumed to be perfect, i.e. without any systematic errors or  
284 random noise. In order to replicate field measurements, the simulated measurement values  
285 were corrupted to generate noisy measurements and bad measurements. Hence, in this sub-  
286 scenario, two types of measurement ambiguities were considered: (i) systematic error, where  
287 a fixed value of 0.2 mg/L is added to a few of the measurements nodes (nodes 19, 25, 27 and  
288 33); (ii) random noise, where a Gaussian noise of mean zero and standard deviation 0.05  
289 mg/L is added to readings from all the measurement nodes. Presence of noise or error in the  
290 measurements usually induces filter inbreeding during data assimilation. Different values of  
291 damping factor  $\alpha$  was used to mitigate the effects of these observational errors.

## 292 **Case Study 2: Bangalore Inflow Network**

293 The second case study is carried out as a verification problem, to validate the algorithm and  
294 to establish its applicability on a large WDS for a big city. The Bangalore water supply  
295 network is maintained and operated by Bangalore Water Supply and Sewerage Board  
296 (BWSSB) and was established by Karnataka Govt. during different time periods: Stage I of  
297 the system was established in year the 1974, Stage 2 was established in year the 1983, Stage  
298 3 (year 1993) and Stage 4 Phase 1 (year 2002). Stage 1 of this network supplies about 140  
299 MLD of water, Stage 2 supplies another 140 MLD, followed by 315 MLD by Stage 3 and  
300 315 MLD by Stage 4 Phase 1, all of it amounting to a total of 910 MLD of water for  
301 Bangalore city. Since the system was established in different stages, zoning of pipes are  
302 carried out for Hazen William C value and wall decay parameter  $k_w$ . Further details of this  
303 network are available in Manohar and Kumar (2013). The hydraulic model of the WDS used  
304 was calibrated using field values.

305 A schematic of Bangalore inflow WDS is given in Fig. 2. In this network, the pipes are  
 306 grouped into 4 different class: pipes 1-41, 42-69, 70-137 and 138-180 and the  $k_w$  values are -1  
 307 (Stage I), -0.75 (Stage II), -0.5 (Stage III) and -0.25 m/day (Stage IV Phase I). The first order  
 308 bulk reaction coefficient is taken as  $2.0 \text{ day}^{-1}$ , and a constant chlorine concentration of 0.75  
 309 mg/L is assumed to be injected from all the four sources (Munavalli and Kumar, 2003 &  
 310 2005). The consumer demands are loaded on the GLRs and are assumed to vary temporally  
 311 based on a bi-modal demand pattern (peak factor: 1.6, and 1.2).

312 A total of 60 measurement nodes are assumed to be present in this network. The chlorine  
 313 measurements were generated once every 15 minutes for a total duration of 16 hours. The  
 314 hydraulic time step is about 60 minutes. As in the case study 1, two different scenarios are  
 315 tested for this network: scenario (i) uncertainty in source concentration ( $C_0$ ) and scenario (ii)  
 316 uncertainty in wall decay coefficients ( $k_{w1}$ ,  $k_{w2}$ ,  $k_{w3}$  and  $k_{w4}$ ) for all the pipe groups. In the  
 317 previous case study, the global wall reaction coefficient is considered ( $k_w$  value same for all  
 318 the pipes in the WDS), where as in this study, a zoned wall reaction coefficient is considered.  
 319 Complexity of this WDS is much higher than the previous case study owing to its size and  
 320 multi-source supply. For this case study, the conclusions drawn from the previous case study  
 321 are used to reduce the computational complexity, and to validate the developed algorithms.

### 322 **Performance criteria**

323 Two different performance measures are used in this study to assess the data assimilation  
 324 accuracy: (i) Average Absolute Error (AAE) and (ii) Average Ensemble Standard Deviation  
 325 (AESD) (Hendricks Franssen and Kinzelback 2008):

$$326 \quad AAE = \frac{1}{M*T} \sum_{i=1}^M \sum_{t=1}^T |\bar{x}_{i,t} - y_{i,t}|, \quad i: 1,2 \dots M \quad (14)$$

$$327 \quad AESD = \frac{1}{M*T} \sum_{i=1}^M \sum_{t=1}^T \sqrt{\frac{\sum_{j=1}^n (x_{i,j,t} - \bar{x}_{i,t})^2}{n}} \quad (15)$$

328 where,  $x$  is the simulated chlorine concentration for each realizations,  $y$  is the measured  
329 chlorine concentration at the node,  $\bar{x}$  indicate the ensemble average value,  $T$  is the total time  
330 of simulation,  $M$  is the number of non-measurement nodes in the WDS and  $n$  indicates the  
331 number of stochastic realizations (number of ensembles) [  $j : 1,2,\dots, n$  ]. Here, AAE and  
332 AESD indicate the overall performance of the EnKF based data assimilation techniques for  
333 the entire time of simulation,  $T$ , for the WDS.

334 Visual comparison based on simulated and measured values of free chlorine at different  
335 measurement nodes in the WDS are also carried out to assess the model performance. Mean  
336 Average Percentage Error (MAPE) for the entire duration of simulation is also calculated to  
337 assess the WDS performance under different scenarios.

## 338 **Results and Discussions**

339 In this section, the results obtained for each case study and the corresponding scenarios are  
340 presented and discussed in detail.

### 341 **Case Study 1: Brushy Plains WDS**

342 Scenario (i) and scenario (ii) were tested for this case study along with sub-scenarios (a), (b)  
343 and (c). The results of this study is presented in the following sections.

#### 344 **Scenario (i): Uncertainty in source chlorine concentrations ( $C_0$ )**

345 The main observations of this study are summarised below:

346 Comparison of NIR-EnKF and IR-EnKF: Fig.3 shows the variation of MAPE for the WDS  
347 for the duration of simulation. It can be deduced from Fig.3, that both NIR-EnKF and IR-  
348 EnKF, reduced the prediction error to 10 % by the end of simulation (IR-EnKF reduced the  
349 MAPE to 5% by the end of simulation). The AAE values estimated at all the nodes in the  
350 WDS for the duration of simulation ranged from 0-0.19mg/L. For this scenario, the



351 difference between NIR-EnKF and IR-EnKF is negligible. It is observed that, IR-EnKF is  
352 slightly more accurate than NIR-EnKF, whereas IR-EnKF takes more computational time  
353 than NIR-EnKF

354 Sub-scenario (a): Simulations are carried for different values of  $n$ , and it is observed that, as  
355 the number of stochastic realizations ( $n$ ) increased, the model output accuracy increased, but  
356 for  $n$  values greater than 20, change in the AAE values are negligible (Table 1). Filter  
357 inbreeding was not observed in any of these simulated results, even for  $n=20$ . As the  $n$  value  
358 was increased from 20 to 100, the estimated AESD values increased for each node for the  
359 duration of simulation. The AESD values are higher than AAE values, for most of the nodes.  
360 This indicates adequate spread of the updated state ensemble. Similar results were observed  
361 in data assimilation studies in the groundwater domain. (Hendriks Franssen and Kinzelbach,  
362 2008). In Hendriks Franssen and Kinzelbach (2008), it was observed that AESD in the  
363 estimated log-transmissivity increased with the number of realizations.

364 Sub-scenario (b): This sub-scenario was simulated for  $n=20$ . In this study, it was found that  
365 the location and number of measurements points were essential for reducing the AAE for the  
366 assimilated quality states in WDS (see Table 1). Fig.4 shows that, measurement set A is able  
367 to assimilate the water quality measurements for the entire WDS, and it is better than  
368 measurement set B, as set B gives higher values of MAPE (around 30-55% higher) at certain  
369 time steps. Among measurement sets A and B, measurement set A is able to estimate chlorine  
370 concentration at almost all the nodes with substantial accuracy. It might be due to the fact  
371 that, set A is very close to the pump station which is a boundary condition for Brushy Plains  
372 WDS, and it is the chlorine source as well.

373 Sub-scenario (c): Table 2. illustrates the effect of damping factor on the model output, in  
374 presence of measurement error and measurement noise. Under  $C_0$  uncertainty,  $\alpha :1$  could

375 handle the measurement errors during data assimilation at all the nodes in the WDS, for the  
376 duration of simulation (Fig. 5(a)),but the AAE for this sub-scenario is higher than the  
377 scenario when no measurement error was present (Table 1).

378 For mitigating the effects of measurement noise in the system, clearly  $\alpha: 1$  is better than all  
379 other values of  $\alpha$  (see Fig.5(b)) .  $\alpha: 0.1$  and  $0.01$  have better model output at a few time steps  
380 (Fig. 5(b) and Table 2). Hence, it can be concluded that for a given WDS, the effect of  
381 measurement noise and measurement error on model performance is negligible and  $n: 20$  is  
382 adequate to simulate the system state at all time periods, without covariance degradation.  
383 The quality of the state estimates were found to be affected by measurement noise and errors,  
384 but  $\alpha: 1$  provides a better estimate of the states compared to other values of the damping  
385 factor. Lower values of  $\alpha$  gives better results during certain time-steps because, at these time-  
386 steps, the impact of spurious numerical co-variances on the updating of states is reduced(i.e.  
387 the value perturbation vector(  $K(Y_t - \hat{Y}_t)$  )is reduced at these time-steps (Hendricks  
388 Franssen and Kinzelbach, 2008).

### 389 **Scenario (ii): Uncertainty in wall reaction coefficient, $k_w$**

390 In this scenario, the wall reaction coefficient is used as the uncertain input to the water  
391 quality data assimilation model. The initial/source chlorine concentration is considered  
392 known (1.1-1.16 mg/L). NIR- EnKF and IR-EnKF methods are compared for chlorine  
393 concentration estimation by assimilating the field measurements under uncertainty in the  $k_w$   
394 value, for different sub-scenarios.

395 Comparison of NIR-EnKF and IR-EnKF: Table 3 summarizes the AAE and AESD for the  
396 WDS, for the duration of study, for different scenarios. Also, the MAPE for the system  
397 reduced to  $< 5\%$  for IR-EnKF at the end of simulation (see Fig.6). It can be observed that IR-  
398 EnKF is better than NIR-EnKF when dealing with uncertainty in the wall reaction coefficient

399 during data assimilation. Due to the nonlinear relationship between the parameter and the  
400 observations, iterative filters are more appropriate for state estimation in WDS under reaction  
401 parameter uncertainty.

402 Sub-scenario (a): The effect of the number of realizations on the model output was similar to  
403 scenario (i). When the number of ensembles was increased from 20-100, AAE values were  
404 found to reduce, but the reduction in AAE is not substantial for  $n > 20$  (Table 3).

405 Sub-scenario (b) : Fig.7 shows the MAPE values of the estimated chlorine concentration for  
406 the WDS under  $k_w$  uncertainty, for measurement set A and measurement set B. It is clear  
407 from Fig.7 that, for every time steps, set A performs better than set B. The overall  
408 performance of the data assimilation technique reduces with reduction in the number of  
409 measurement nodes.

410 Sub-scenario (c) : It was found that model performance was unaffected by measurement  
411 error, though  $\alpha: 1$  and  $\alpha: 0.1$  had similar response at all nodes, at all time-steps (Table 2.).  
412 When measurement noise was introduced, it was found that,  $\alpha: 0.1$ , performed better than  $\alpha: 1$   
413 for most of the time-steps (see Fig.8(b)), but the improvement in model performance was not  
414 substantial (the change in MAPE was about 1-2%). Hence, it can be deduced that, noise or  
415 error induced degeneration of the covariance matrix was not much in this WDS for  $n: 20$ .

416 Based on the results from sub-scenario (c) (for both scenario (i) and scenario (ii)), it is  
417 observed that measurement noise and measurement error is not creating large variations in  
418 the perturbation vector (when compared with the case when no measurement error or noise is  
419 considered) [perturbation vector :  $K(Y_t - \hat{Y}_t)$ ]. But, it should be noted that , measurement  
420 error and measurement noise reduced the accuracy of the data assimilation model (Table 1,  
421 Table 2 and Table 3).

## 422 **Estimated Parameter Values**

423 Table 4 show the computed mean values for the parameters,  $C_0$  and  $k_w$  at the end of the  
424 simulation period. Mean values were computed for the simulation where  $n$ : 20. It is clear  
425 from the results that, data assimilation technique based on EnKF can be used for dynamic  
426 state estimation and parameter estimation ( $C_0$  and  $k_w$ ) in WDS under various uncertainty and  
427 measurement location scenarios. The values obtained using data assimilation techniques were  
428 found to be comparable to parameters estimated using inverse modelling methodologies  
429 (Munavalli and Kumar, 2005).

### 430 **Case Study 2: Bangalore Inflow System**

431 In this case study, data from 60 measurement nodes (30 network junctions and 30 tanks) were  
432 assimilated with the network water quality model. The number and location of these 60  
433 measurement nodes were chosen heuristically for an optimal concentration estimation across  
434 the WDS. Initially, 10 nodes were assigned across the network at random, such that they are  
435 uniformly distributed across the network. Data assimilation was carried out (for scenario (i)) ,  
436 and based on the error in estimation of nodal chlorine concentration, nodes with higher error  
437 values were added to the measurement node set. The measurement nodes were added such  
438 that, no two measurements nodes were adjacent. Similar procedure was carried out for  
439 deciding the measurements tanks as well. The locations chosen include 30 tanks and 30  
440 junctions spread across the network. Fig.9 shows the variation of AAE with  $m$  value for this  
441 study. It was found that, as  $m$  value increased, the error in estimation reduced, but the  
442 reduction in error was not substantial after certain  $m$  value. For in-depth understanding of the  
443 sensitivity of the number and location of measurements nodes on the data assimilation model  
444 accuracy, a detailed analysis need to be carried out. A detailed sensitivity analysis is beyond  
445 scope of this paper, and will be carried out in future works.

446 In this analysis, the tank measurements were used to assimilate the chlorine concentration  
447 values at the tanks and junction measurements were used to assimilate the chlorine  
448 concentration data at the junctions in the network, and the tank and junction states are  
449 updated simultaneously. The conclusions drawn from the previous case study was utilized  
450 here, as this case study is considered as a validation problem for water quality data  
451 assimilation application in large scale WDS. Scenario (i) and scenario (ii) are considered for  
452 this case study. The number of stochastic realizations,  $n$  is 50 , for this case study, since it  
453 was observed that the AESD and AAE values do not change significantly for values of  $n >$   
454 50. No measurement errors are considered in this WDS. In this case study, the performance  
455 indicators (AAE and AESD) are slightly modified, since these values are calculated for each  
456 node, and are not averaged over all non-measurement nodes (i.e. in equation (14) and (15),  
457 averaging over  $M$  is not considered).

#### 458 **Scenario (i): Uncertainty in source concentration ( $C_0$ )**

459 NIR-EnKF is used for state estimation in this scenario. Fig.10 show the AAE (mg/L) for non-  
460 measurement nodes and tanks in the WDS. It can be observed that NIR-EnKF is able to  
461 estimate the chlorine concentration estimate of the network with an AAE accuracy of about  
462 0.005 - 0.2 mg/L. It is observed that the AAE values at nodes upstream and downstream of  
463 valves and pumps were generally higher (AAE  $>$  0.2 mg/L) compared to the error estimates  
464 at other nodes. This is due to the hydraulic modelling constraint associated with the forward  
465 simulation model. In the forward simulation model adopted (EPANET) in this work, valves  
466 and pumps are modelled as network links without length, i.e. the nodes upstream and  
467 downstream of these links are hypothetical. Due to of this constraint, the variation in flow  
468 velocity across the valves and pumps, generates an estimate of chlorine concentration, which  
469 is higher than the actual value. All the remaining nodes have AAE value below 0.18 mg/L,  
470 and about 75% of the nodes have AAE value below 0.12 mg/L (Fig.10). AAE for chlorine

471 estimates at the tanks of this network were found to be below 0.2 mg/L for all the non-  
472 measurement tanks (Fig.10). This high level of accuracy might be due to a high measurement  
473 density with respect to tanks in the network. In Fig. 10, AAE values are presented only at the  
474 non-measurement nodes in the figure; Measurement nodes, and the nodes upstream and  
475 downstream of valves and pumps are not shown in the figure.

#### 476 **Scenario (ii): Uncertainty in wall decay coefficient ( $k_w$ )**

477 IR-EnKF was used to estimate the water quality state under uncertainty in reaction coefficient  
478 for case study 2. The  $k_w$  parameters were zoned in the network according to the pipe age  
479 (dependent on the phase of development of the WDS). In this case study, IR-EnKF is able to  
480 estimate the chlorine concentration at the tanks and nodes of this network with an accuracy of  
481  $\leq 0.2$ mg/L. Fig.11 shows the AAE for all the non-measurement nodes and tanks in the WDS  
482 (AAE values are not reported at the measurement nodes, and the nodes upstream and  
483 downstream of valves and pumps in the figure). It was observed that the number of nodes  
484 with AAE  $\sim 0.2$  mg/L is greater than the previous scenario. Frequent flow reversal occurs in  
485 many pipes in this WDS, which along with disparity in  $k_w$  value across the system contributed  
486 to a higher value of AAE in many nodes. As many as 36 nodes in the system have AAE  
487 values almost equal to 0.2 mg/L. More than 75% of the nodes in this system have AAE  
488 value below 0.18 mg/L and it was observed that the tank estimates for chlorine concentration  
489 are good and all the tanks have AAE  $< 0.2$  mg/L.

#### 490 **Estimated Parameter Values**

491 The parameter values estimated at the end of the simulation are given in Table 5. The  
492 ensemble mean value of  $C_0$  was calculated to be 0.7534 mg/L. Mean value for  $k_{w2}$  and  $k_{w3}$   
493 were: -0.7784 and -0.504 m/d respectively. The  $k_{w1}$  value for this case study was estimated to  
494 be lesser than the actual value, whereas,  $k_{w4}$  value was estimated to be higher than the actual

495 value. Frequent flow reversal happens in pipes in group 1 ( $k_{w1}$ ) and group 4 ( $k_{w4}$ ), and  
496 grouping of pipes solely based on the service age, are the reasons for this disparity between  
497 actual and estimated  $k_{w1}$  and  $k_{w4}$  values. The estimated values are compared with the steady  
498 state-inverse modelling study carried out by Munavalli and Mohan Kumar (2003) on an  
499 earlier version of the network, which had only Stage 1, 2 and 3. From these results it is  
500 concluded that the data assimilation method is able to achieve the same level of accuracy as  
501 that of inverse modelling.

## 502 **Summary and Conclusions**

503 This work introduces a novel method for estimating chlorine concentration across a WDS in  
504 real time using data assimilation techniques. Two variants of the EnKF are studied and  
505 applied on two WDS. The major conclusions drawn from this study are stated in this section.

506 In this study, it was found that, the uncertainty in the source concentration can be dealt by  
507 both NIR-EnKF and IR-EnKF. However, the computational time required for NIR-EnKF  
508 method is lesser than IR-EnKF based data assimilation method.

509 It was found that, the non-linear relationship between the parameters and the measurements  
510 cannot be addressed with non-iterative data assimilation methods, hence IR-EnKF was more  
511 accurate than NIR-EnKF for data assimilation in presence of  $k_w$  uncertainty. For both the case  
512 studies, the data assimilation approach was able to accurately estimate the dynamic state and  
513 parameter of the system under different input parameter uncertainties-  $C_0$  uncertainty and  $k_w$   
514 uncertainty.

515 The NIR-EnKF and IR-EnKF based data assimilation technique were able to reach the good  
516 output accuracy across Brushy plains network, for state estimation under uncertainty in  $C_0$   
517 and  $k_w$ . Since case study 2 was developed in stages, , the pipes in the WDS were grouped  
518 based on wall reaction coefficients, to estimate accurate values of the chlorine concentrations

519 across the system. The results of this case study illustrate the capability of EnKF based  
520 assimilation methods to deal with system uncertainties irrespective of the size of the  
521 network. The limited sensitivity analysis carried out in this study showed the variation of  
522 model accuracy with the number and location of measurement nodes. For an in-depth  
523 understanding of the sensitivity of the number and location of measurements nodes on the  
524 data assimilation model, a detailed sensitivity analysis need to be carried out.

525 With regard to the field application of this method, the model output will be influenced by  
526 uncertainties in the hydraulic model of the system. Uncertainties related to the hydraulic  
527 model induces additional non-linearity, in the forward simulation model, hence, the output of  
528 the proposed data assimilation methods could become sub-optimal. Also, response of the data  
529 assimilation methods when the water quality reaction equation is of different order is not  
530 considered in this study. The data assimilation models will be sensitive to the order of water  
531 quality reactions, hence uncertainty in the order of reaction equation will also reduce the  
532 model accuracy. The results obtained in this paper could certainly be improved if these  
533 system constraints are also considered.

## 534 **References**

535 Al-Jasser, A. O. (2007). "Chlorine decay in drinking-water transmission and distribution  
536 systems: Pipe service age effect." *Water Res.*, 41(2), 387-396.

537 Anderson, J. L. (2007). "An adaptive covariance inflation error correction algorithm for  
538 ensemble filters." *Tellus A*, 59(2), 210-224.

539 Anderson, J. L., and Anderson, S. L. (1999). "A Monte Carlo implementation of the  
540 nonlinear filtering problem to produce ensemble assimilations and forecasts." *Monthly*  
541 *Weather Review*, 127(12), 2741-2758.



542 Aral, M. M., Guan, J., and Maslia, M. L. (2009). "Optimal design of sensor placement in  
543 water distribution networks." *J. of Water Resour.Plann. and Manage.*, 136(1), 5-18.

544 Baxter, C. W., Stanley, S. J., and Zhang, Q. (1999). "Development of a full-scale artificial  
545 neural network model for the removal of natural organic matter by enhanced coagulation." *J.*  
546 *Water Supply: Res. and Tech.-AQUA*, 48(4), 129-136.

547 Baxter, C. W., Zhang, Q., Stanley, S. J., Shariff, R., Tupas, R. R., and Stark, H. L. (2001).  
548 "Drinking water quality and treatment: the use of artificial neural networks." *Canadian J. of*  
549 *Civil Engg.*, 28(S1), 26-35.

550 Beides, H. M., and Heydt, G. T. (1991). "Dynamic state estimation of power system  
551 harmonics using Kalman filter methodology." *IEEE Transactions on Power Delivery*, 6(4),  
552 1663-1670.

553 Benkherouf, A., and Allidina, A. Y. (1988, March). "Leak detection and location in gas  
554 pipelines." In *IEE Proceedings D-Control Theory and Applications* (Vol. 135, No. 2, pp.  
555 142-148). IET.

556 Biswas, P., Lu, C., and Clark, R. M. (1993). "A model for chlorine concentration decay in  
557 pipes." *Water Res.*, 27(12), 1715-1724.

558 Blood, E. A., Krogh, B. H., and Ilic, M. D. (2008, July). "Electric power system static state  
559 estimation through Kalman filtering and load forecasting." In *Power and Energy Society*  
560 *General Meeting-Conversion and Delivery of Electrical Energy in the 21st Century, 2008*  
561 *IEEE* (pp. 1-6). IEEE.

562 Boccelli, D. L., Tryby, M. E., Uber, J. G., Rossman, L. A., Zierolf, M. L., and Polycarpou,  
563 M. M. (1998). "Optimal scheduling of booster disinfection in water distribution systems." *J.*  
564 *of Water Resour.Plann. and Manage.*, 124(2), 99-111.

565 Bowden, G. J., Nixon, J. B., Dandy, G. C., Maier, H. R., and Holmes, M. (2006).  
566 “Forecasting chlorine residuals in a water distribution system using a general regression  
567 neural network.” *Mathematical and Computer Model.*, 44(5-6), 469-484.

568 Burgers, G., Jan van Leeuwen, P., and Evensen, G. (1998). Analysis scheme in the ensemble  
569 Kalman filter. *Monthly Weather Rev.*, 126(6), 1719-1724.

570 Carton, J. A., and Giese, B. S. (2008). A reanalysis of ocean climate using Simple Ocean  
571 Data Assimilation (SODA).” *Monthly Weather Rev.*, 136(8), 2999-3017.

572 Clark, R. M. (2015). “The USEPA's distribution system water quality modelling program: a  
573 historical perspective.” *Water and Envi. J.*, 29(3), 320-330.

574 Clark, R. M., Grayman, W. M., Males, R. M., and Hess, A. F. (1993). “Modeling  
575 contaminant propagation in drinking-water distribution systems.” *J. of Envi.Engg.*, 119(2),  
576 349-364.

577 Clark, R. M., Rossman, L. A., and Wymer, L. J. (1995). “Modeling distribution system water  
578 quality: Regulatory implications.” *J. of Water Resour.Plann. and Manage.*, 121(6), 423-428.

579 D D'Souza, C., and Kumar, M.S.M. (2010). “Comparison of ANN models for predicting  
580 water quality in distribution systems.” *American Water Works Association. J.*, 102(7), 92.

581 Doucet, A., Gordon, N. J., and Krishnamurthy, V. (2001). “Particle filters for state estimation  
582 of jump Markov linear systems.” *IEEE Transactions on signal processing*, 49(3), 613-624.

583 Drécourt, J. P., Madsen, H., and Rosbjerg, D. (2006). “Calibration framework for a Kalman  
584 filter applied to a groundwater model.” *Adv. in Water Resour.*, 29(5), 719-734.

585 Emara-Shabaik, H. E., Khulief, Y. A., and Hussaini, I. (2002). “A non-linear multiple-model  
586 state estimation scheme for pipeline leak detection and isolation.” *Proceedings of the*

587 *Institution of Mechanical Engineers, Part I: Journal of Systems and Control*  
588 *Engineering*, 216(6), 497-512.

589 Evensen, G. (1994). "Sequential data assimilation with a nonlinear quasi- geostrophic model  
590 using Monte Carlo methods to forecast error statistics." *J. of Geophysical Res.:  
591 Oceans*, 99(C5), 10143-10162.

592 Evensen, G. (2003). "The ensemble Kalman filter: Theoretical formulation and practical  
593 implementation." *Ocean Dynamics*, 53(4), 343-367.

594 Fisher, I., Kastl, G., and Sathasivan, A. (2017). "New model of chlorine-wall reaction for  
595 simulating chlorine concentration in drinking water distribution systems." *Water Res.*, 125,  
596 427-437.

597 Geir, N., Johnsen, L. M., Aanonsen, S. I., and Vefring, E. H. (2003, January). "Reservoir  
598 monitoring and continuous model updating using ensemble Kalman filter." In *SPE Annual  
599 Technical Conference and Exhibition*. Society of Petroleum Engineers.

600 Gibbs, M. S., Morgan, N., Maier, H. R., Dandy, G. C., Nixon, J. B., and Holmes, M. (2006).  
601 "Investigation into the relationship between chlorine decay and water distribution parameters  
602 using data driven methods." *Mathematical and Computer Model.*, 44(5-6), 485-498.

603 Grayman, W. M., Clark, R. M., and Males, R. M. (1988). "Modeling distribution-system  
604 water quality; dynamic approach." *J. of Water Resour.Plann. and Manage.*, 114(3), 295-312.

605 Gu, Y., and Oliver, D. S. (2007). "An iterative ensemble Kalman filter for multiphase fluid  
606 flow data assimilation." *SPE J.*, 12(04), 438-446.

607 Hall, J., Zaffiro, A. D., Marx, R. B., Kefauver, P. C., Krishnan, E. R., Haught, R. C., and  
608 Herrmann, J. G. (2007). "On-line water quality parameters as indicators of distribution  
609 system contamination." *J.American Water Works Assoc.*, 99(1), 66-77.

610 Hallam, N. B., West, J. R., Forster, C. F., Powell, J. C., and Spencer, I. (2002). "The decay of  
611 chlorine associated with the pipe wall in water distribution systems." *Water Res.*, 36(14),  
612 3479-3488.

613 Hamill, T. M., Mullen, S. L., Snyder, C., Baumhefner, D. P., and Toth, Z. (2000). "Ensemble  
614 forecasting in the short to medium range: Report from a workshop." *Bulletin of the American*  
615 *Meteorological Society*, 81(11), 2653-2664.

616 Hart, W. E., and Murray, R. (2010). "Review of sensor placement strategies for  
617 contamination warning systems in drinking water distribution systems." *J. of Water*  
618 *Resour.Plann. and Manage.*, 136(6), 611-619.

619 Hendricks Franssen, H. J., and Kinzelbach, W. (2008). "Real- time groundwater flow  
620 modeling with the ensemble Kalman filter: Joint estimation of states and parameters and the  
621 filter inbreeding problem". *Water Resour. Res.*, 44(9).

622 Houtekamer, P. L., and Mitchell, H. L. (1998). "Data assimilation using an ensemble Kalman  
623 filter technique." *Monthly Weather Review*, 126(3), 796-811.

624 Hutton, C. J., Kapelan, Z., Vamvakeridou-Lyroudia, L., andSavić, D. A. (2012). "Dealing  
625 with uncertainty in water distribution system models: A framework for real-time modeling  
626 and data assimilation." *J. of Water Resour.Plann. and Manage.*, 140(2), 169-183.

627 Jung, D., and Lansey, K. (2014). "Water distribution system burst detection using a nonlinear  
628 Kalman filter." *J. of Water Resour.Plann. and Manage.*, 141(5), 04014070.

629 Kalman, R. E. (1960). "A new approach to linear filtering and prediction problems." *J. of*  
630 *Basic Engg.*, 82(1), 35-45.

631 Kalnay, E. (2003). "*Atmospheric modeling, data assimilation and predictability*". Cambridge  
632 university press.

633 Kang, D., and Lansey, K. (2009). "Real-time demand estimation and confidence limit  
634 analysis for water distribution systems." *J.ofHyd.Engg.*, 135(10), 825-837.

635 Larson, T. E. (1966). "Deterioration of water quality in distribution systems." *J-American*  
636 *Water Works Assoc.*, 58(10), 1307-1316.

637 Liu, M., Zang, S., and Zhou, D. (2005). "Fast leak detection and location of gas pipelines  
638 based on an adaptive particle filter." *International Journal of Applied Mathematics and*  
639 *Computer Science*, 15(4), 541.

640 Liu, Y., Weerts, A., Clark, M., Hendricks Franssen, H. J., Kumar, S., Moradkhani, H., Seo,  
641 D-J., Schwanenberg, D., Smith, P., van Dijk, A.I.J.M., van Velzen, N., He, M., Lee, H., Noh,  
642 S.J., Rakovec, O., and Restrepo, P. (2012). "Advancing data assimilation in operational  
643 hydrologic forecasting: progresses, challenges, and emerging opportunities." *Hyd. and Earth*  
644 *Sys. Sci.*, 16, 3863.

645 Lorenc, A. C. (2003). "The potential of the ensemble Kalman filter for NWP- a comparison  
646 with 4D- Var." *Quarterly Journal of the Royal Meteorological Society*, 129(595), 3183-  
647 3203.

648 Maier, H. R., Morgan, N., and Chow, C. W. (2004). "Use of artificial neural networks for  
649 predicting optimal alum doses and treated water quality parameters." *Envi.Model.&*  
650 *Software*, 19(5), 485-494.

651 Manohar, U., and Mohan Kumar, M. S.M. (2013). Modeling equitable distribution of water:  
652 Dynamic inversion-based controller approach. *J. of Water Resour.Plann. and*  
653 *Manage.*, 140(5), 607-619.

654 May, R. J., Dandy, G. C., Maier, H. R., and Nixon, J. B. (2008). "Application of partial  
655 mutual information variable selection to ANN forecasting of water quality in water  
656 distribution systems." *Envi.Model. & Software*, 23(10-11), 1289-1299.

657 Milot, J., Rodriguez, M. J., and Sérodes, J. B. (2002). "Contribution of neural networks for  
658 modeling trihalomethanes occurrence in drinking water." *J. of Water Resour.Plann. and*  
659 *Manage.*, 128(5), 370-376.

660 Moradkhani, H., Sorooshian, S., Gupta, H. V., and Houser, P. R. (2005). "Dual state–  
661 parameter estimation of hydrological models using ensemble Kalman filter." *Adv. in Water*  
662 *Resour.*, 28(2), 135-147.

663 Munavalli, G.R. (2002), *Simulation and parameter estimation of water quality in water*  
664 *distribution system*, PhD Thesis, Indian Institute of Science, Bangalore, India.

665 Munavalli, G. R., and Kumar, M. S. M. (2003). "Water quality parameter estimation in  
666 steady-state distribution system". *J. of Water Resour. Plann. and Manage.*, 129(2), 124-134.

667 Munavalli, G. R., and Kumar, M. S. M. (2004). "Modified Lagrangian method for modeling  
668 water quality in distribution systems." *Water Res.*, 38(13), 2973-2988.

669 Munavalli, G. R., and Kumar, M. M. (2005). "Water quality parameter estimation in a  
670 distribution system under dynamic state." *Water Res.*, 38(13), 2973-2988.

671 Naevdal, G., L. V. Johnsen, S. I. Aanonsen, and E. H. Vefring (2003). "Reservoir monitoring  
672 and continuous model updating using ensembleKalman filter." *Soc. Petrol.*, 84372.

673 Nilsson, K. A., Buchberger, S. G., and Clark, R. M. (2005). Simulating exposures to  
674 deliberate intrusions into water distribution systems. *J. of Water Resour. Plann. and*  
675 *Manage.*, 131(3), 228-236.

676 Okeya, I., Kapelan, Z., Hutton, C., and Naga, D. (2014). "Online modelling of water  
677 distribution system using data assimilation." *Procedia Engineering*, 70, 1261-1270.

678 Ostfeld, A., Uber, J. G., Salomons, E., Berry, J. W., Hart, W. E., Phillips, C. A., and di  
679 Pierro, F. (2008). "The battle of the water sensor networks (BWSN): A design challenge for  
680 engineers and algorithms." *J. of Water Resour.Plann. and Manage.*, 134(6), 556-568.

681 Park, J. H., and Kaneko, A. (2000). "Assimilation of coastal acoustic tomography data into a  
682 barotropic ocean model." *Geophysical Research Letters*, 27(20), 3373-3376.

683 Pasha, M. F., and Lansey, K. (2010). "Effect of Parameter Uncertainty on Water Quality in  
684 Distribution Systems – Case study," *J. of Hydroinformatics*, 12(1),doi:  
685 10.2166/hydro.2010.053.

686 Pastres, R., Ciavatta, S., andSolidoro, C. (2003). "The Extended Kalman Filter (EKF) as a  
687 tool for the assimilation of high frequency water quality data.: *Ecological modelling*, 170(2-  
688 3), 227-235.

689 Polycarpou, M. M., Uber, J. G., Wang, Z., Shang, F., and Brdys, M. (2002). "Feedback  
690 control of water quality." *IEEE Control Systems*, 22(3), 68-87.

691 Rodriguez, M. J., and Sérodes, J. B. (1998). "Assessing empirical linear and non-linear  
692 modelling of residual chlorine in urban drinking water systems." *Envi. Model.&*  
693 *Software*, 14(1), 93-102.

694 Rossman, L. A. (2000). *EPANET 2: User's manual*. Cincinnati, OH, US-EPA.

695 Rossman, L. A., Boulos, P. F., and Altman, T. (1993). "Discrete volume-element method for  
696 network water-quality models." *J. of Water Resour.Plann. and Manage.*, 119(5), 505-517.

697 Rossman, L. A., Clark, R. M., and Grayman, W. M. (1994). "Modeling chlorine residuals in  
698 drinking-water distribution systems." *J. of Envi.Engg.*, 120(4), 803-820.

699 Sérodes, J. B., Rodriguez, M. J., and Ponton, A. (2001). “Chlorcast©: a methodology for  
700 developing decision-making tools for chlorine disinfection control.” *Env.Model. &*  
701 *Software, 16(1)*, 53-62.

702 Simone, A., Giustolisi, O., and Laucelli, D. B. (2016). “A proposal of optimal sampling  
703 design using a modularity strategy.” *Water Resour. Res.*, 52(8), 6171-6185.

704 Song, X., Shi, L., Ye, M., Yang, J., and Navon, I. M. (2014). “Numerical comparison of  
705 iterative ensemble Kalman filters for unsaturated flow inverse modeling.” *Vadose Zone*  
706 *Journal, 13(2)*.

707 Soyupak, S., Kilic, H., Karadirek, I. E., and Muhammetoglu, H. (2011). “On the usage of  
708 artificial neural networks in chlorine control applications for water distribution networks with  
709 high quality water.” *J. of Water Supply: Res. and Tech.-Aqua, 60(1)*, 51-60.

710 Suresh, M., Manohar, U., Anjana, G.R , Stoleru, R., and Kumar, M. S. M.(2014, October). “A  
711 cyber-physical system for continuous monitoring of Water Distribution Systems.” In *Wireless*  
712 *and Mobile Computing, Networking and Communications (WiMob), 2014 IEEE 10th*  
713 *International Conference on* (pp. 570-577). IEEE.

714 van Loon, M., Builtjes, P. J., and Segers, A. J. (2000). “Data assimilation of ozone in the  
715 atmospheric transport chemistry model LOTOS.” *Envi.Model. & Software, 15(6-7)*, 603-609.

716 Vasconcelos, J. J., Rossman, L. A., Grayman, W. M., Boulos, P. F., and Clark, R. M. (1997).  
717 Kinetics of chlorine decay.” *J.American Water Works Assoc.*, 89(7), 54.

718 Whitaker, J. S., and Hamill, T. M. (2002). “Ensemble data assimilation without perturbed  
719 observations.” *Monthly Weather Rev.*, 130(7), 1913-1924.

720 Ye, G., and Fenner, R. A. (2010). “Kalman filtering of hydraulic measurements for burst  
721 detection in water distribution systems.” *J of Pipeline Sys. Engg. and Prac.*, 2(1), 14-22.



722 Ye, G., and Fenner, R. A. (2013). "Weighted least squares with expectation-maximization  
723 algorithm for burst detection in UK water distribution systems." *J. of Water*  
724 *Resour.Plann.and Manage.*, 140(4), 417-424.

725 **FIGURE CAPTIONS:**

726 Fig. 1. Schematic of Brushy plains WDS - Case study 1

727 Fig. 2. Schematic of Bangalore Inflow System - Case study 2 (with Tanks and Junction ID)

728 Fig. 3. MAPE for the case study 1 under  $C_0$  uncertainty [ $n$ : 20,  $m$ : 8]

729 Fig. 4: MAPE for the case study 1 under  $C_0$  uncertainty for  $m$ : 4 [ $n$ :20, using NIR-EnKF]

730 Fig. 5. MAPE for case study 1 under  $C_0$  uncertainty (a) different  $\alpha$  for measurement error[0.2

731 mg/L]; (b) different  $\alpha$  for measurement noise [Gaussian]; [ $n$  :20 and  $m$ : 8, using NIR-EnKF]

732 Fig. 6. MAPE for case study 1 under  $k_w$  uncertainty [ $n$ : 20,  $m$ : 8]

733 Fig. 7. MAPE for case study 1 under  $k_w$  uncertainty, for  $m$  :4 [ $n$ : 20, using IR-EnKF]

734 Fig. 8. MAPE for case study 1 under  $k_w$  uncertainty (a) different  $\alpha$  for measurement error [

735 0.2 mg/L]; (b) different  $\alpha$  for measurement noise [Gaussian]; [ $n$  :20 and  $m$ : 8, using IR-

736 EnKF]

737 Fig.9. AAE plots for different  $m$  values ( case study 2 - under  $C_0$  uncertainty, using NIR-

738 EnKF )

739 Fig. 10. AAE (mg/L) for non-measurement nodes and tanks in case study 2, using NIR-EnKF

740 [ $n=50,m=60$ ]

741 Fig. 11. AAE (mg/L) for non-measurement nodes and tanks in case study 2, using IR-EnKF

742 [ $n=50,m=60$ ]

743 **Tables**

744 **Table 1. Performance of EnKF algorithms for different scenarios where  $C_0$  is uncertain**

No. of Measurements	Method	No. of Realizations, $n$	AAE (mg/L)	AESD(mg/L)
8	NIR-EnKF	20	0.071	0.159
	NIR-EnKF	50	0.064	0.167
	NIR-EnKF	100	0.06	0.17
8	IR-EnKF	20	0.065	0.124
	IR-EnKF	50	0.058	0.126
	IR-EnKF	100	0.058	0.131
4-A	NIR-EnKF	20	0.078	0.173
	NIR-EnKF	50	0.076	0.183
	NIR-EnKF	100	0.069	0.181
4-B	NIR-EnKF	20	0.124	0.185
	NIR-EnKF	50	0.112	0.192
	NIR-EnKF	100	0.111	0.193

745

746 **Table 2. Average Absolute Error (AAE (mg/L)) calculated for different scenarios and  $\alpha$  values for dealing with**  
 747 **measurement ambiguity during data assimilation**

Parameter	$\alpha$ Value	Measurement error (AAE in mg/L)	Measurement noise (AAE in mg/L)
$C_0$	1	0.083	0.239
	0.1	0.358	0.375
	0.01	0.225	0.2
	0.001	0.566	0.334
$k_w$	1	0.063	0.064
	0.1	0.07	0.058
	0.01	0.138	0.126
	0.001	0.078	0.146

748

749

750

751

752

753

754

755

756

757

Table 3. Performance of EnKF algorithms for different scenarios where  $k_w$  is uncertain

No. of Measurements	Method	No. of Realizations, $n$	AAE (mg/L)	AESD(mg/L)
8	NIR-EnKF	20	0.175	0.075
	NIR-EnKF	50	0.157	0.08
	NIR-EnKF	100	0.157	0.08
8	IR-EnKF	20	0.056	0.075
	IR-EnKF	50	0.055	0.079
	IR-EnKF	100	0.054	0.08
4-A	IR-EnKF	20	0.063	0.081
	IR-EnKF	50	0.06	0.082
	IR-EnKF	100	0.06	0.085
4-B	IR-EnKF	20	0.08	0.101
	IR-EnKF	50	0.71	0.105
	IR-EnKF	100	0.69	0.107

758

759

760

Table 4. Computed mean value of the parameters at the end of simulation for case study 1 (n:20) for different scenarios (Method inside the bracket is the method used for the parameter estimation)

Parameter	True Value	NIR-EnKF	IR-EnKF	Measurement set A (Method)	Measurement set B (Method)	Measurement Error (Method)	Measurement Noise (Method)	Literature (Inverse Modelling)
$C_0$ (mg/L)	1.15	1.124	1.087	1.147 (NIR-EnKF)	1.297 (NIR-EnKF)	1.169 (NIR-EnKF)	1.131 (NIR-EnKF)	Not Available
$k_w$ (m/d)	-0.3	-1.538	-0.272	-0.211 (IR-EnKF)	-0.347 (IR-EnKF)	-0.228 (IR-EnKF)	-0.276 (IR-EnKF)	-0.365*

761

\*Munavalli and Kumar, 2005

762

763

Table 5. Computed mean value of the parameters at the end of simulation for case study 2 (n:50) for different scenarios

Parameter	Unit	Observed Value	Computed Ensemble Mean	Inverse Modelling
$C_0$	mg/L	0.75	0.753	0.71 <sup>#</sup>
$k_{w1}$	m/d	-1	-0.842	-1.1066*
$k_{w2}$	m/d	-0.75	-0.766	-0.7993*
$k_{w3}$	m/d	-0.5	-0.503	-0.4924*
$k_{w4}$	m/d	-0.25	-0.327	Not Available

764

765

766

767

\*Munavalli and Kumar, 2003

<sup>#</sup> Munavalli, 2002

Figure 1

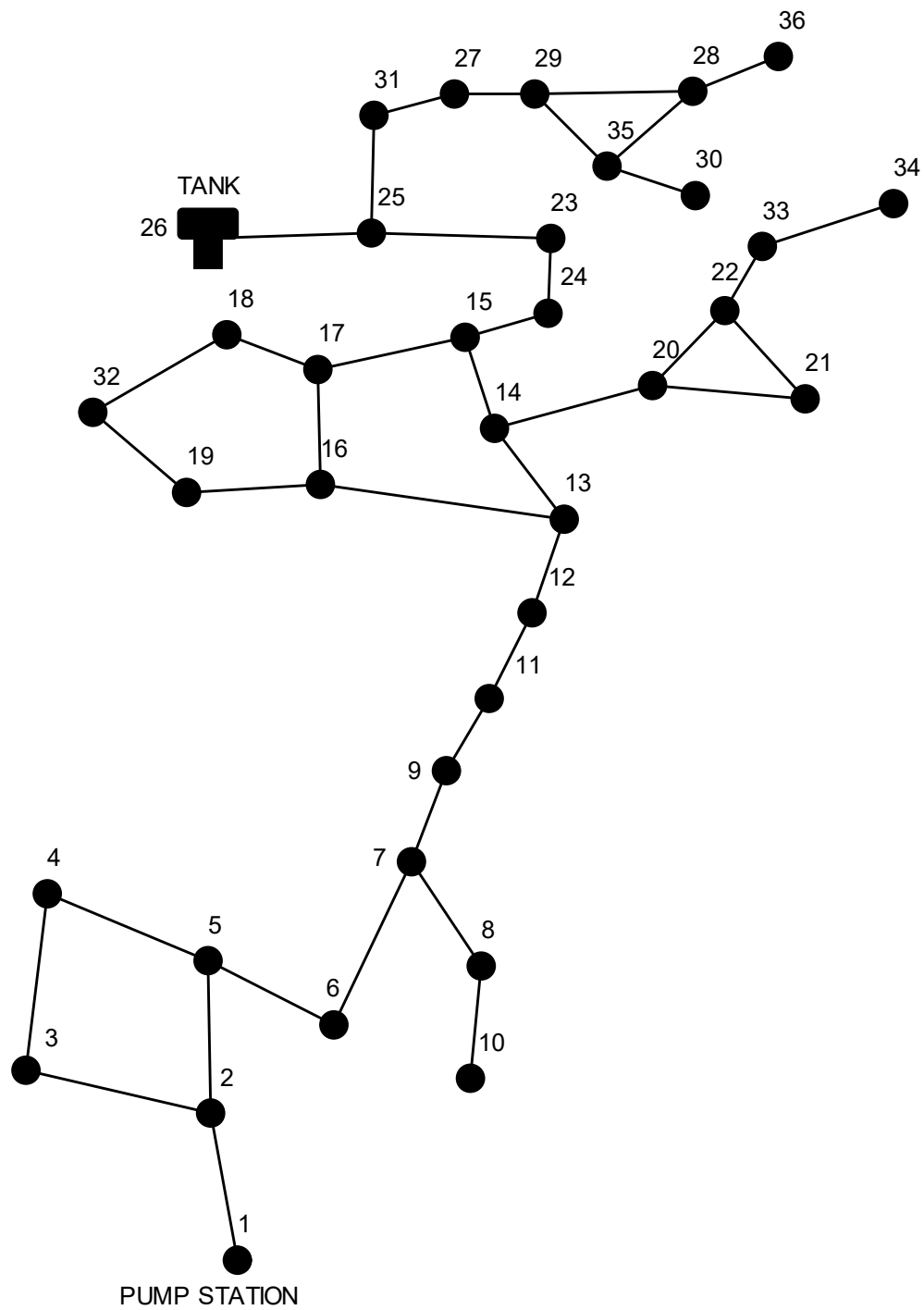


Figure 2

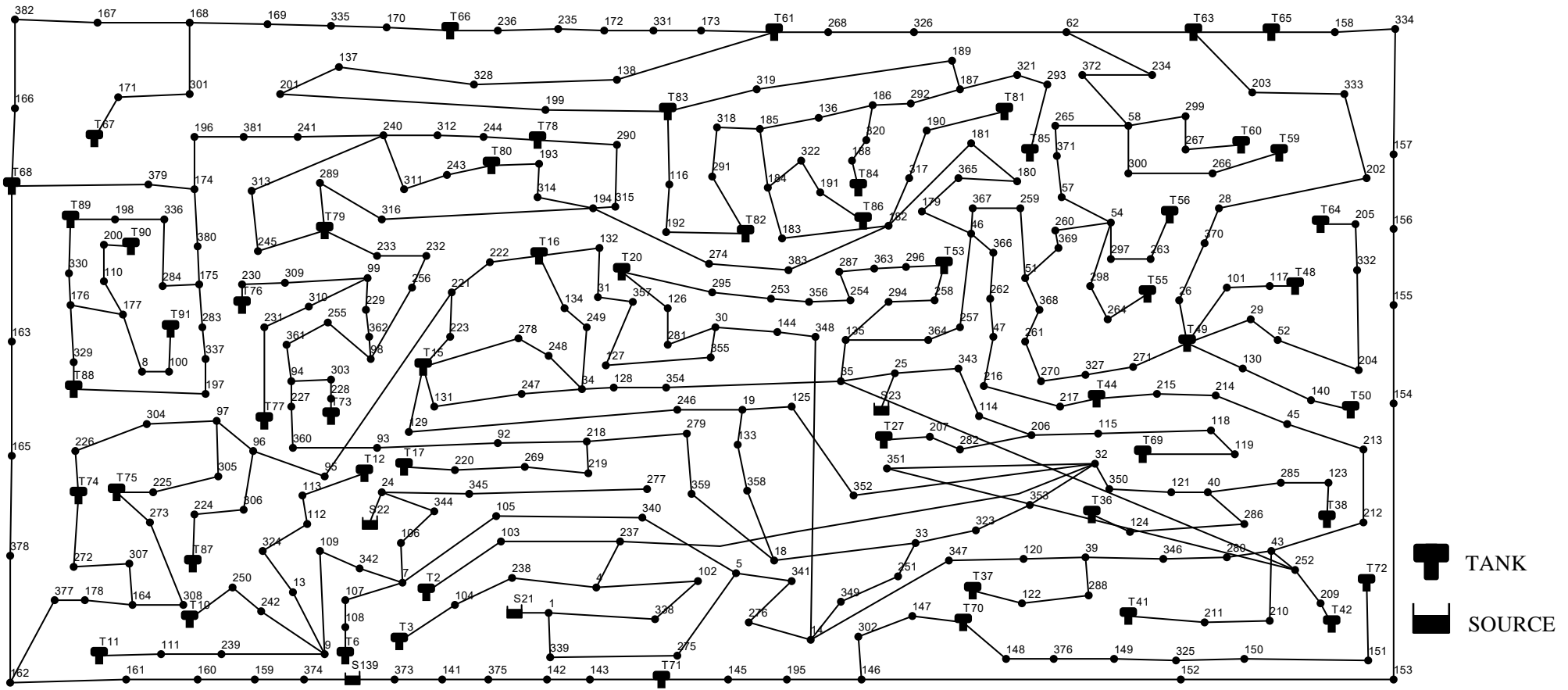


Figure 3

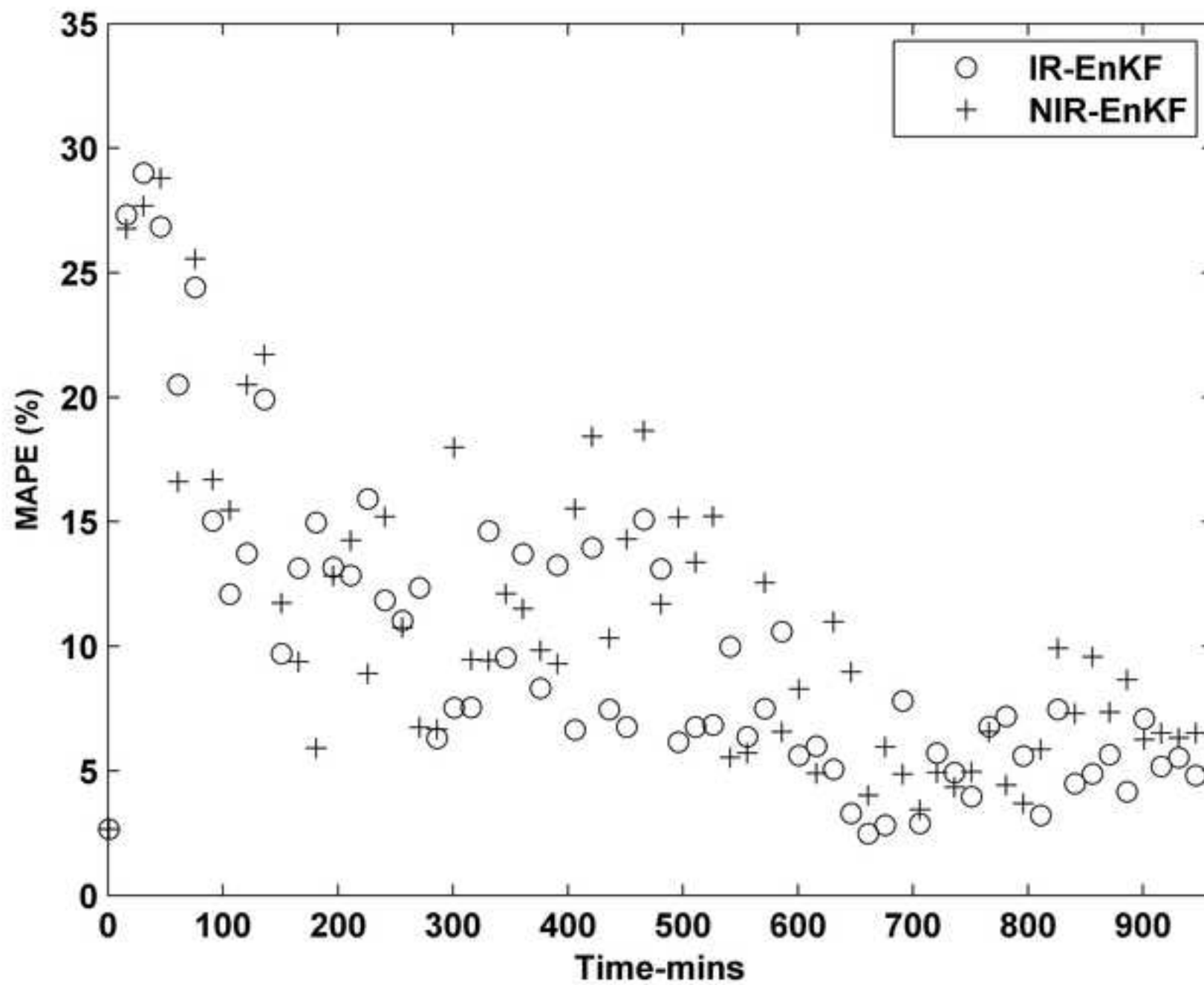
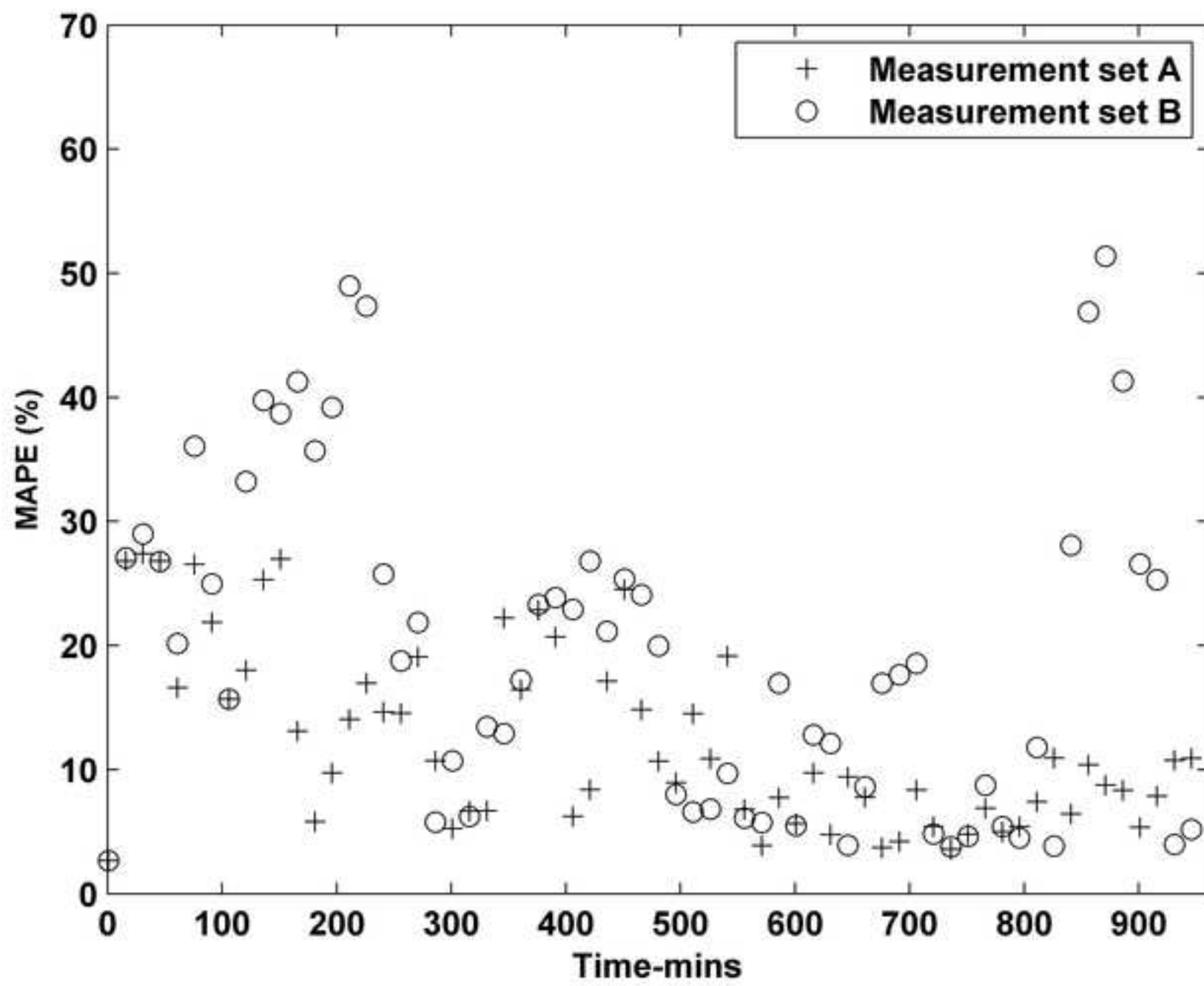
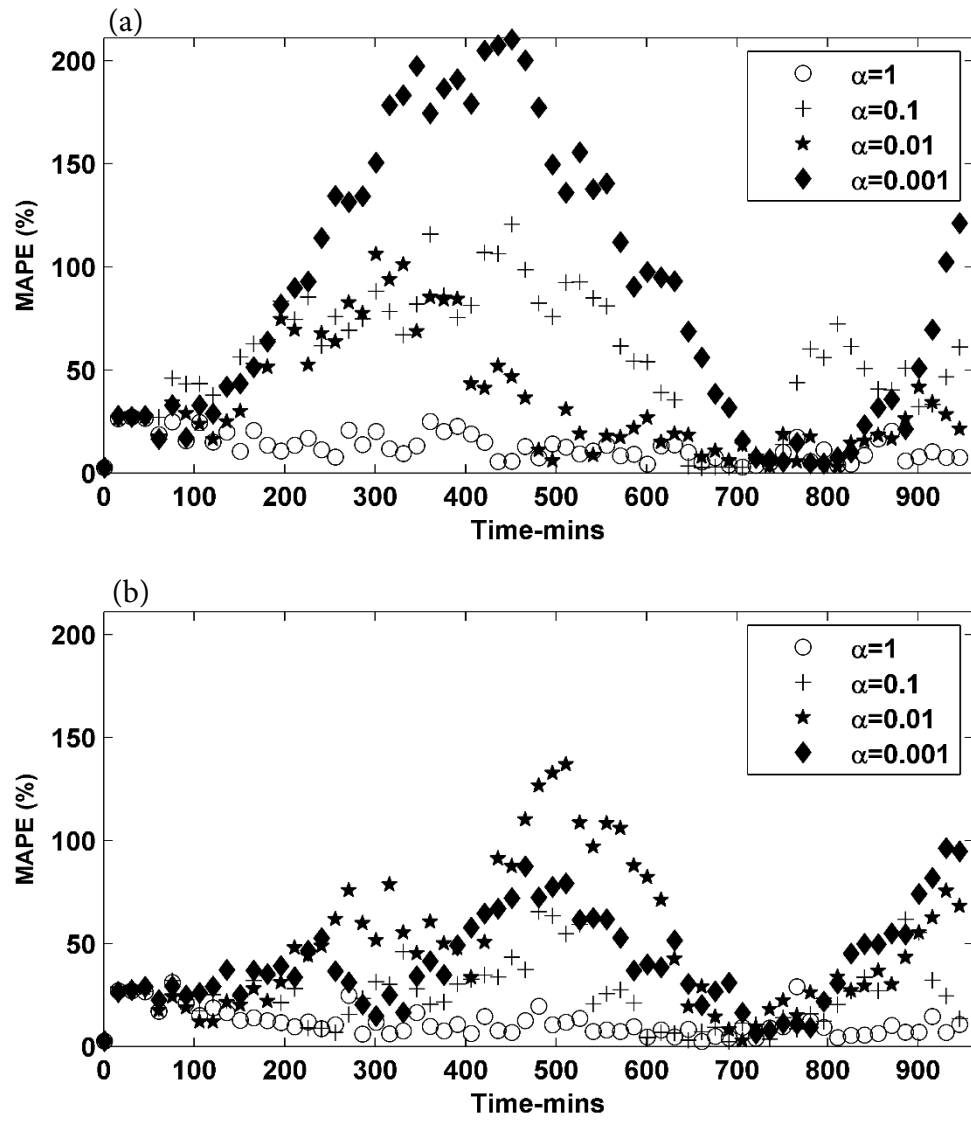
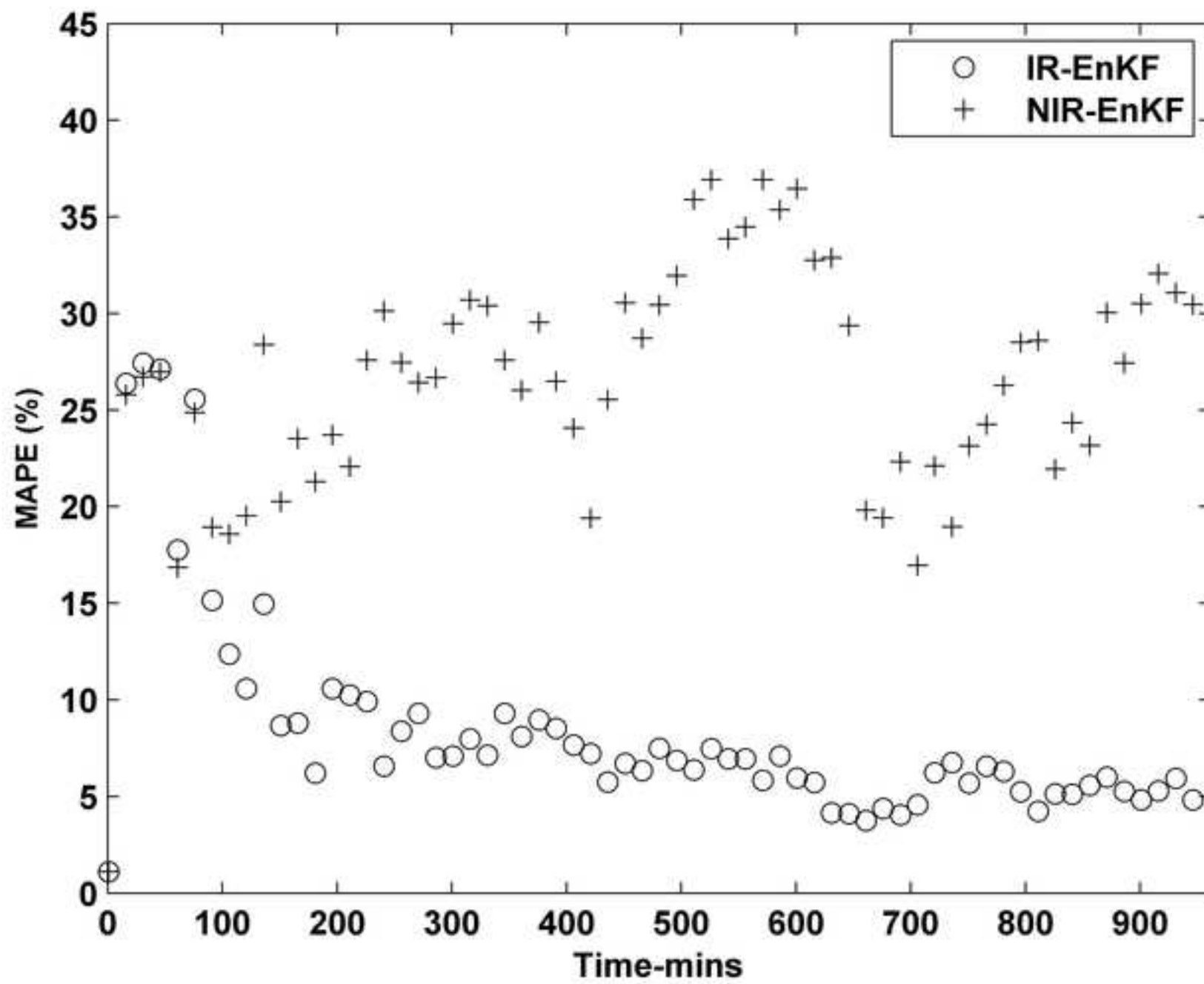


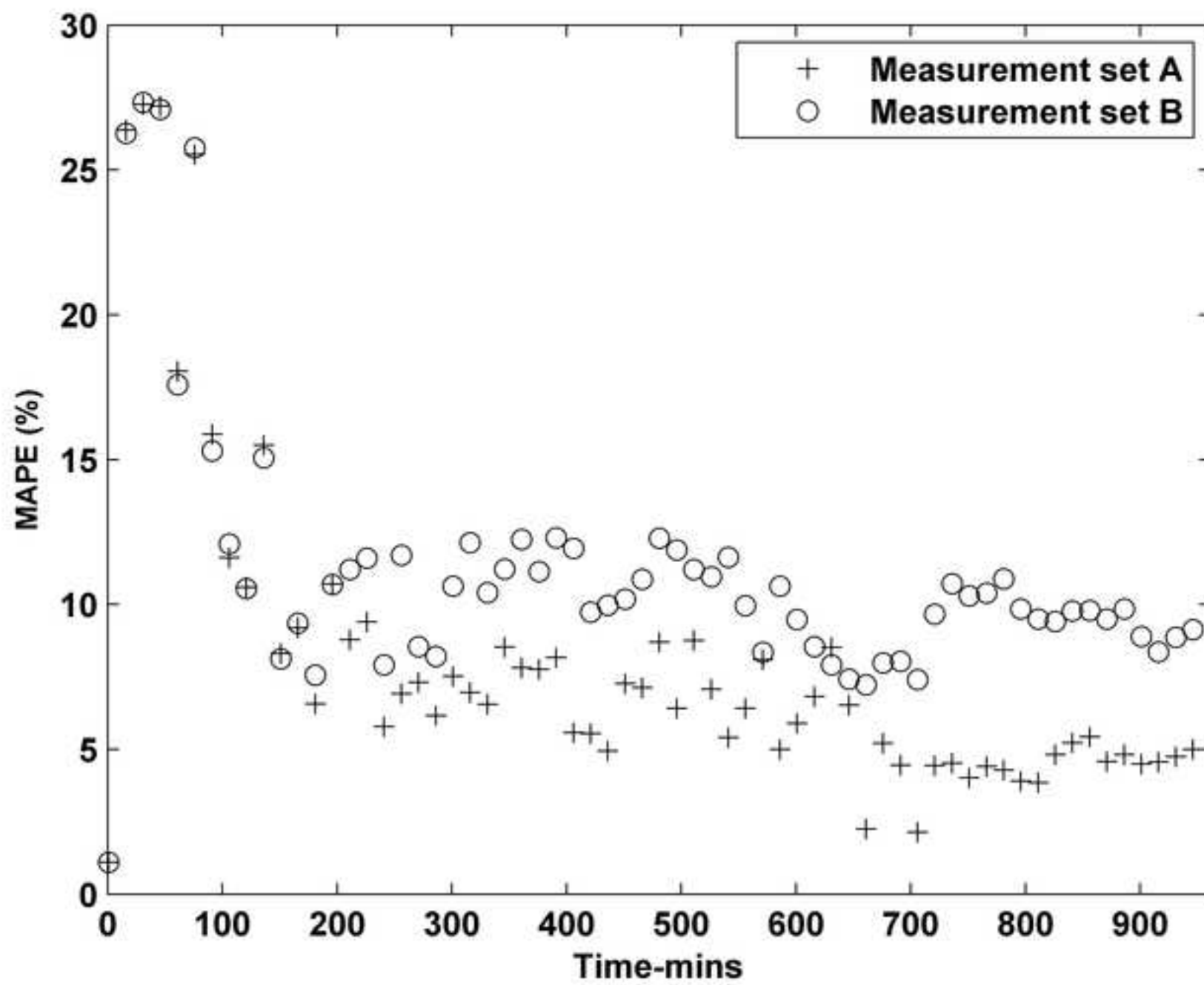
Figure 4

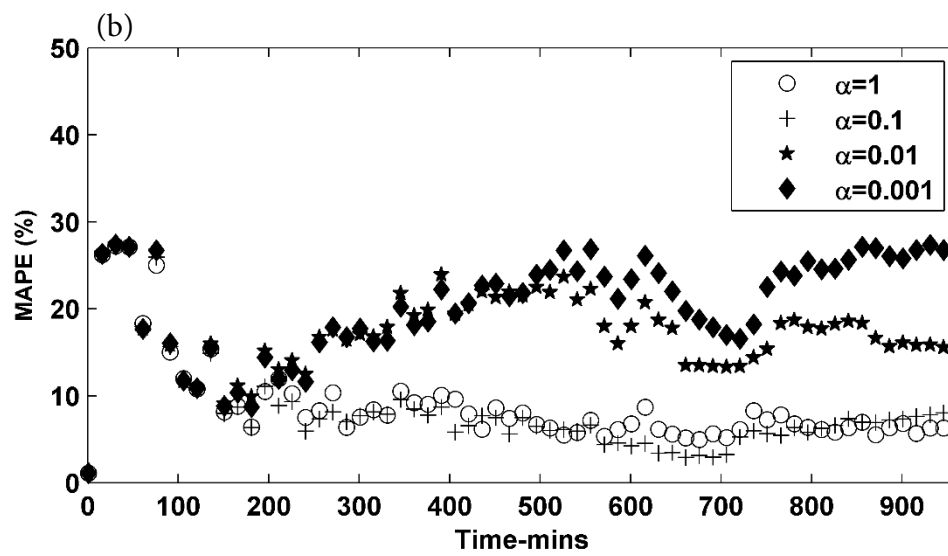
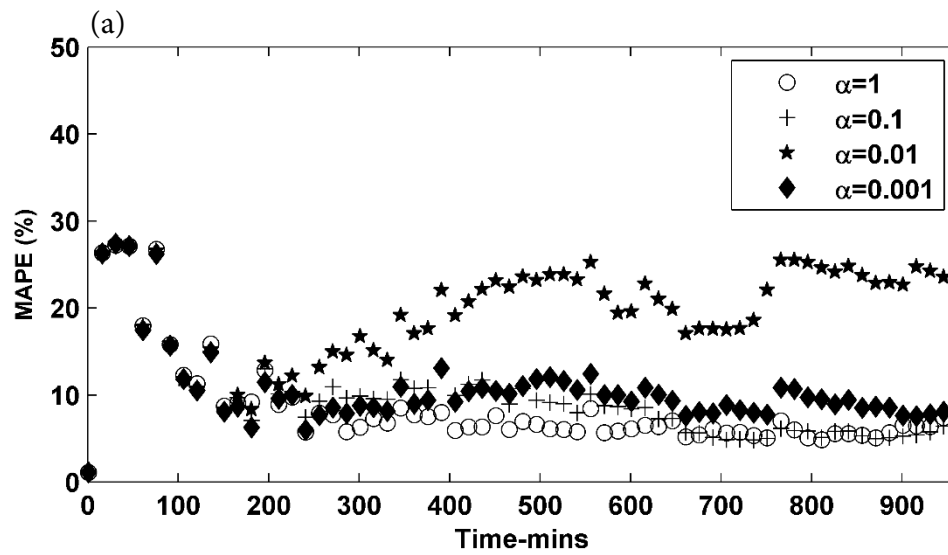












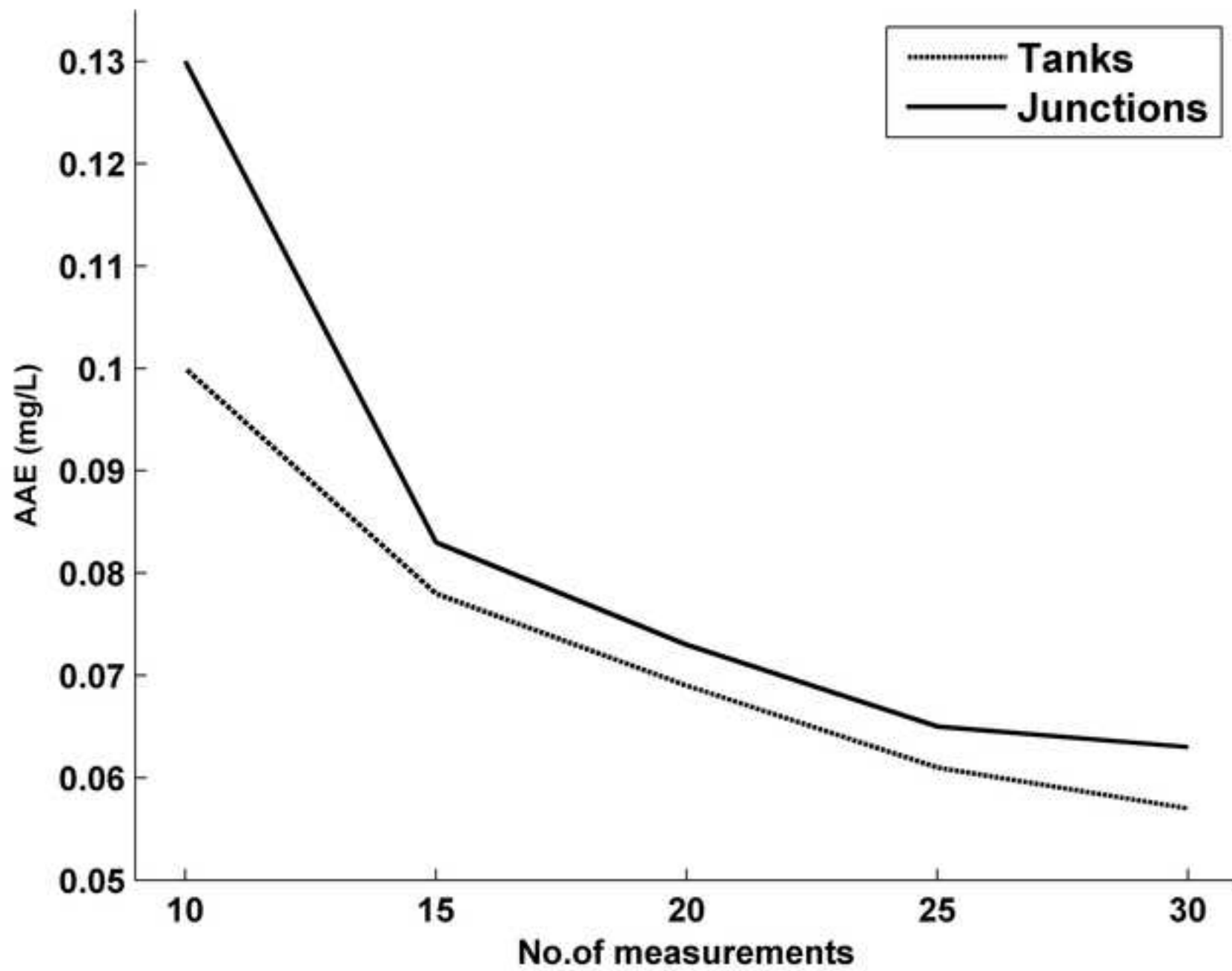


Figure 10

